

Supporting Information

Addition of *N*-nucleophiles to gold(III)-bound isocyanides leading to short-lived gold(III) acyclic diaminocarbene complexes

Tatyana B. Anisimova,^a Mikhail A. Kinzhalov,^b M. Fátima C. Guedes da Silva,^a
Alexander S. Novikov,^b Vadim Yu. Kukushkin,^b Armando J. L. Pombeiro,^{*a} and
Konstantin V. Luzyanin^{*b,c}

^aCentro de Química Estrutural, Instituto Superior Técnico, Universidade de Lisboa, Av. Rovisco Pais, 1049-001 Lisbon, Portugal, e-mail: pombeiro@tecnico.ulisboa.pt

^bSaint Petersburg State University, 7/9 Universitetskaya Nab., Saint Petersburg 199034, Russian Federation

^cDepartment of Chemistry, University of Liverpool, Crown Street, Liverpool L69 7ZD, United Kingdom, e-mail: konstantin.luzyanin@liverpool.ac.uk

Content

Experimental section	3
Materials and instrumentation	3
X-ray structure determinations	3
Computational details	5
Preparation of gold(III)-isocyanide complexes 5–8	6
Characterization of gold(III)-isocyanide complexes 5–8	7
DFT calculations for model isocyanide complexes [AuCl ₃ (CNMe)] and [AuCl(CNMe)]	11
Addition of benzophenone hydrazone to gold(III)-bound isocyanides	13
Characterization of the prepared carbene complexes 14–16	14
Reaction of [AuCl ₃ (CNR ¹)] (5–8) with amines	17
Characterization of 12	19
Reactions of [AuCl ₃ (CNR ¹)] (5–8) with other NH-nucleophiles	22
Theoretical evaluation of the bonding situation in dimers 5 , 14 , and (<i>R</i>)- 12	23
Cartesian atomic coordinates of model species	27

Experimental Section

Materials and instrumentation

HAuCl₄•3H₂O, the isocyanides, and all nucleophiles were obtained from Aldrich and used as received without further purification. Tetrahydrothiophene, salicylaldehyde and 9-fluorenone hydrazones were purchased from Alfa Aesar, and benzophenone imine was purchased from Acros. All solvents and HCl were ordered from Fisher Chemical and were used without further purification apart from CH₂Cl₂ that was dried over P₂O₅ or CaCl₂ and distilled. The complexes [AuCl(CNR¹)]¹ (**1–4**) were synthesized accordingly to the previously reported methods. C, H, N elemental analyses were carried out by the Microanalytical Service of the Instituto Superior Técnico. ESI^{+/-} mass spectra were measured on a Varian 500-MS LC ion trap mass spectrometer (IST-Node) and a Bruker micrOTOF ESI-MS-spectrometer (Saint Petersburg State University) in MeCN, MeOH, or CH₂Cl₂ as the solvents. ¹H, ¹³C{¹H} and all the 2D NMR spectra were recorded on a Bruker Avance II+ 400 MHz spectrometer at ambient temperature.

X-ray structure determinations

Crystals were mounted in Nylon loops with small amount of cryo-oil, and measured at 150 K. Intensity data were collected using a Bruker AXS-KAPPA APEX II diffractometer with graphite monochromatic Mo-K α (λ 0.71073) radiation. Data were collected using omega scans of 0.5° per frame and full sphere of data was obtained. Cell parameters were retrieved using Bruker SMART software and refined using Bruker SAINT² on all the observed reflections. Absorption corrections were applied using SADABS.³ Structures were solved by direct methods by using the SHELXS-97³ package and refined with SHELXL-2013.³ Calculations were performed using the WinGX System–Version 2013.03.⁴ The hydrogen

atoms were located from the difference Fourier synthesis but inserted at geometrically calculated positions and included in the refinement using the riding-model approximation. CCDC1471327–1471329 contain the supplementary crystallographic data for this paper. These data can be obtained free of charge from The Cambridge Crystallographic Data Centre via www.ccdc.cam.ac.uk/data_request/cif.

Table S1. Crystal Data and Structure Refinement Details for **5**, **14•CHCl₃** and **(R)-12**.

	5	14•CHCl₃	(R)-12
Empirical formula	C ₉ H ₉ AuCl ₃ N	C ₂₃ H ₂₂ AuCl ₆ N ₃	C ₁₆ H ₂₄ AuCl ₅ N ₂
Formula weight	434.49	750.10	618.59
Crystal system	Monoclinic	Monoclinic	Orthorhombic
space group	P 21/n	P 21/c	C 2 2 21
<i>a</i> (Å)	8.2328(3)	10.0454(10)	8.9036(5)
<i>b</i> (Å)	13.6539(6)	14.1896(12)	21.1337(13)
<i>c</i> (Å)	10.9324(5)	19.4905(18)	26.6726(16)
<i>α</i> (deg)	90	90	90
<i>β</i> (deg)	102.002(2)	93.721(5)	90
<i>γ</i> (deg)	90	90	90
<i>V</i> (Å ³)	1202.05(9)	2772.3(4)	5018.9(5)
<i>Z</i>	4	4	8
No. rfls.	9451	24691	16434
Rfls Unique/Obs	2465/2051	5061/3945	5012/3613
ρ_{calc} (Mg/m ³)	2.401	1.797	1.637
μ (Mo K α) (mm ⁻¹)	12.866	5.902	6.396
<i>R</i> _{int}	0.0425	0.0582	0.0711
Final <i>R</i> ₁ ^a , <i>wR</i> ₂ ^b (<i>I</i> ≥ 2 σ)	0.0301, 0.0703	0.0305, 0.0589	0.05300, 0.1278
GOF	1.117	1.022	1.013

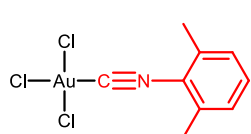
$$^a R_1 = \frac{\sum ||F_o| - |F_c||}{\sum |F_o|}, \quad ^b wR_2 = \left[\frac{\sum [w(F_o^2 - F_c^2)^2]}{\sum [w(F_o^2)^2]} \right]^{1/2}$$

Computational details

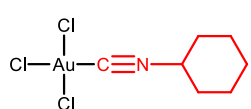
The single point calculations for dimeric clusters **5**, **14**, and **(R)-12** have been carried out at DFT level of theory using the M06 functional⁵ (this functional was specifically developed to describe weak dispersion forces and non-covalent interactions) with the help of *Gaussian-09*⁶ program package. The experimental X-ray geometries were used as starting points. Two approaches were used, viz. (i) the Douglas–Kroll–Hess 2nd order scalar relativistic calculations⁷ requested relativistic core Hamiltonian were carried out using DZP-DKH basis sets⁸ for all atoms; (ii) the non-relativistic calculations were carried out using a quasi-relativistic Stuttgart pseudopotential that described 60 core electrons and the appropriate contracted basis set for the gold atoms⁹ and the 6-311+G* basis sets for other atoms. The topological analysis of the electron density distribution with the help of the QTAIM method developed by Bader¹⁰ has been performed by using the Multiwfn program¹¹ (version 3.3.4). The Wiberg bond indices (WI) were computed by using the natural bond orbital (NBO) partitioning scheme.¹² The full geometry optimization of [AuCl₃(CNMe)] and [AuCl(CNMe)] structures have been also carried out at DFT level of theory using the M06 functional⁵ with the help of *Gaussian-09*⁶ program package using a quasi-relativistic Stuttgart pseudopotential that described 60 core electrons and the appropriate contracted basis set for the gold atoms⁹ and the 6-311+G* basis sets for other atoms. No symmetry operations have been applied and Hessian matrix was calculated analytically for the optimized structures in order to prove the location of correct minima (no imaginary frequencies). The Cartesian atomic coordinates of all model species are given in **Table S3**.

Preparation of [AuCl₃(CNR₁)] (5–8)

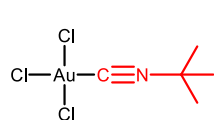
An excess of dry gaseous chlorine was bubbled through a solution of [AuCl(CNR¹)] (R¹ = Cy **1**, Xyl **2**, Bu^t **3**, (*S*)-CHMePh **4**) (0.1 mmol) in dry CH₂Cl₂ (2 mL) at 20 °C for ca. 30 sec. Solutions of the thus formed [AuCl₃(CNR¹)] (R¹ = Xyl **5**, Cy **6**, Bu^t **7**, (*S*)-CHMePh **8**) were evaporated to dryness under a flow of N₂ at RT (20–25 °C) giving target compounds as bright yellow solids (**5–7**, 96–99% isolated yields) or a yellow oil (**8**, 83%). Crystals of **5** suitable for X-ray diffraction were prepared by slow evaporation of its CH₂Cl₂ solution at RT under dinitrogen.



[AuCl₃(CNXyl)] (5, yellow solid, 99%). Elemental analyses were not conclusive due to slow decomposition of compound at RT. MS (ESI⁻) *m/z*: [M + Cl + 2MeCN + H₂O]⁻ calcd. for C₁₃H₁₇N₃AuCl₄O 570, found: 570; [M + Cl + H₂O]⁻ calcd. for C₉H₁₁AuCl₄NO: 488, found: 488; [M - CNXyl + Cl]⁻ calcd. for AuCl₄: 339, found: 339. FT-IR (KBr, selected bands, cm⁻¹): 3050–2917 (w, C–H), 2268 (m, C≡N). ¹H NMR (CD₂Cl₂, δ): 7.51 (t, ³J_{HH} 7.7 Hz, 1H, *p*-CH), 7.32 (d, ³J_{HH} 7.7 Hz, 2H, *m*-CH), 2.57 ppm (s, 6H, Me). ¹³C {¹H} NMR (CD₂Cl₂, δ): 138.0 (*p*-CH), 133.1 (*o*-C), 128.8 (*m*-CH), 18.2 (Me), C–N≡C carbons were not detected due to the poor solubility and low stability in CD₂Cl₂.



[AuCl₃(CNCy)] (6, yellow solid, 96%). Anal. calcd for C₇H₁₁NCl₃Au: C 20.38, H 2.69 N, 3.40%, found: C 20.32, H 2.61, N 3.20%. MS (ESI⁻) *m/z*: [M + Cl]⁻ calcd. for C₇H₁₁NAuCl₄: 448, found: 448. FT-IR (KBr, selected bands, cm⁻¹): 2945, 2928 and 2860 (s, C–H), 2297 (s, C≡N). ¹H NMR (CD₂Cl₂, δ): 4.38–4.30 (m, 1H, CH), 2.15–1.90 and 1.87–1.73 (2m, 4H+2H, α- and γ-CH₂), 1.65–1.50 ppm (m, 4H, β-CH₂). ¹³C {¹H} NMR (CD₂Cl₂, δ): 111.8 (t, ¹J_{NC} 33 Hz, CN), 58.0 (CH), 30.9 (α-CH₂), 24.3 (β-CH₂), 22.2 (γ-CH₂).



[AuCl₃(CNBu^t)] (7, yellow solid, 96%). Anal. calcd for

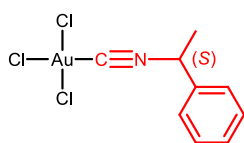
C₅H₉NCl₃Au•0.5CHCl₃: C 14.81, H 2.15, N 3.14%; found: C 14.67,

H 2.12, N, 3.37%. MS (ESI⁻) *m/z*: [M + Cl]⁻ calcd. for 422, found: 422;

[M - CNBu^t + Cl]⁻ calcd. for AuCl₄: 339, found: 339. FT-IR (KBr, selected bands,

cm⁻¹): 2987 (s, C-H), 2291 (s, C≡N). ¹H NMR (CDCl₃, δ): 1.71 ppm (s, 9H, Me).

¹³C {¹H} NMR (CDCl₃, δ): 112.1 (t, ¹J_{NC} 29 Hz, CN), 63.6 (C), 29.4 (Me).



[AuCl₃{CN((S)-CHMePh)}] (8, bright yellow oil, 83%).

Elemental analyses were not performed due to an oily body of the compound. MS (ESI⁺) *m/z*: [M - Cl]⁻ calcd. for C₉H₉NAuCl₂: 398,

found: 398. FT-IR (KBr, selected bands, cm⁻¹): 3033, 2996, 2936 and 2872 (w, C-H),

2308 (s, C≡N). ¹H NMR (CDCl₃, δ): 7.57–7.47 (m, 3H, *m*- and *p*-C_{Ar}H), 7.44 (d,

³J_{HH} 6.5 Hz, 2H, *o*-C_{Ar}H), 5.45 (quart, ³J_{HH} 6.7 Hz, 1H, NCH), 1.99 ppm (d,

³J_{HH} 6.7 Hz, 3H, Me). ¹³C {¹H} NMR (CDCl₃, δ): 133.8 (C_{Ar}), 130.3 (C_{Ar}H), 129.9

(C_{Ar}H), 125.8 (C_{Ar}H), 114.0 (t, ¹J_{CN} 31.0 Hz, C≡N), 59.9 (CH), 23.2 (Me).

Characterization of gold(III)-isocyanide complexes 5–8

All isocyanides complexes **5–8** were characterized by ESI⁻-MS, IR, ¹H and ¹³C {¹H} NMR spectroscopic techniques, while complexes **6** and **7** additionally by (C, H, N) elemental analysis, and **5** by single-crystal X-ray diffraction.

Complexes **6** and **7** gave satisfactory results of the C, H and N elemental analyses which are consistent with the proposed formulations of the (isocyanide)Au^{III} complexes [AuCl₃(CNR¹)]. In the case of **5** and **8**, elemental analyses were unsatisfactory owing to their fast decomposition even in darkness under N₂ atmosphere.

For complex **5**, signals due to [M + Cl + H₂O]⁻, [M + Cl + H₂O + 2MeCN]⁻ in the ESI⁻-MS, due to [M - Cl + H₂O + 2MeCN]⁻ in the ESI⁺-MS were observed. For complexes **6** and

7, signals due to $[M + Cl]^-$ ions were evident in the ESI⁻-MS spectra. For complex **8**, fragmentation ions $[M - Cl]$ and $[M - Cl - CNCHMePh]$ in the ESI⁺-MS, were identified.

The IR spectra of **5–8** contained one strong (**6–8**) or medium (**5**) band in the range 2268–2297 cm^{-1} that was attributed to $\nu(\text{C}\equiv\text{N})$ stretching vibrations. These values are higher than those for the corresponding Au^I compounds $[\text{AuCl}(\text{CNR}^1)]$ (2308–2259 cm^{-1} for $\text{R}^1 = \text{Cy, Xyl, Bu}'$, and (*S*)-CHMePh)^{1, 13} suggesting that that Au(III) center provides higher electrophilic activation of the isocyanide ligands when compared to Au(I). Observed values are comparable to those for $\nu(\text{C}\equiv\text{N})$ stretches of the known complex $[\text{AuBr}_3(\text{CNBu}'^1)]$ (2282 cm^{-1})¹⁴. Bands in the 3050–2860 cm^{-1} range are characteristic for $\nu(\text{C-H})$ stretches.

In the ¹H NMR spectrum of **5**, the methyl group from the Xyl fragment emerged as a singlet at 2.57 ppm, that is shifted by *ca.* 0.1 ppm to a lower field when compared to the corresponding Au^I complex **1** (2.47 ppm). In the ¹H NMR spectrum of **6**, the CH proton of the cyclohexyl ring was detected in the range of 4.38–4.30 ppm as a broad multiplet (3.86–3.94 ppm for **2**). The characteristic signal of the asymmetric group CH appeared in the ¹H NMR spectrum of **8** as a quartet at 5.45 ppm (³*J*_{HH} 6.7 Hz); this value is low-field shifted by *ca.* 0.35 ppm regarding starting complex **4**.

In the ¹³C{¹H} NMR spectrum of **5**, the methyl group emerged at 18.2 ppm, while the CN group was not detected due to its low intensity and fast decomposition of **5** in solution (all the signals detected in the spectrum were shifted to lower field compared to $[\text{AuCl}(\text{CNXyl})]^1$). In the ¹³C{¹H} NMR spectrum of **6**, the CH carbon of the cyclohexyl group appeared at 58.0 ppm as a singlet (55.0 ppm for **2**), CN group was found at 111.8 ppm as a triplet (¹*J*_{NC} 33 Hz), while for **2** the latter was not detected. In the ¹³C{¹H} NMR spectrum of **7**, the CN carbon was detected as a triplet at 112.1 ppm (¹*J*_{NC} 29 Hz). Carbon resonances of the CH and C≡N groups of complex **8** appeared as a singlet and a triplet at 59.9 and 114.0 ppm (¹*J*_{CN} 31.0 Hz), correspondingly.

The solid-state structure of **5** was established by single-crystal X-ray diffraction (Figures S1 and S2). Complex **5** possesses a square-planar geometry ($\tau_4 = 0.03$)¹⁵ with the metal coordination environment comprising one isocyanide and three chloride ligands. The Au–Cl [Au1–Cl1 2.2687(19), Au1–Cl2 2.2837(18), and Au1–Cl3 2.2868(18) Å] and Au–C [1.954(7) Å] distances are of typical values and similar to those in related Au(III) and Au(I) compounds.^{14, 16} For the *trans*-placed chloride ligands, the Au–Cl distances are slightly longer than for the remaining *cis*-chloride, presumably, due to the greater *trans* influence of the CNR ligands than that of Cl.¹⁷ The C1–N1 bond [1.143(9) Å] is a typical CN triple bond for the isocyanide moieties.¹⁸ The Au–C1–N1–C2 fragment is almost linear and the molecule of **5** is roughly planar as shown by the angle (7.41°) between the least-square planes of the aromatic ring and the AuCl₃ group. Molecules of **5** are gathered into dimers as a result of Au1•••Cl3 intermolecular contacts of 3.353(2) Å (Figure S2) leading to a shortest metal•••metal distance of 3.9797(4) Å. Detailed theoretical evaluation of the character of these gold-halogen contacts by using DFT calculations followed by the topological analysis of the electron density distribution within the formalism of Bader's theory (QTAIM analysis) is provided below.

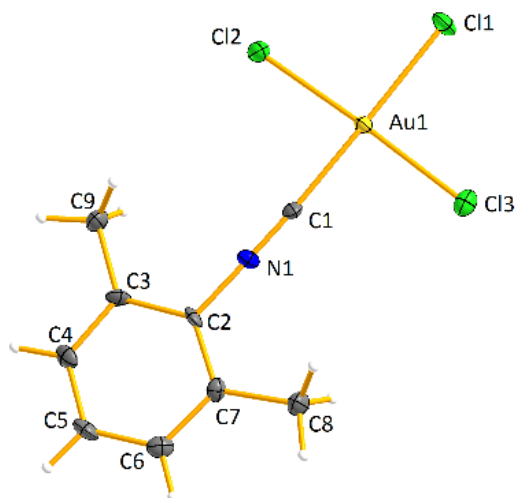


Figure S1. Crystal structure of **5** with the atomic numbering scheme (hydrogen labels are removed for simplicity). Thermal ellipsoids are drawn at the 25% probability level. Selected bond lengths (Å) and angles (°): Au1–Cl1 2.2687(19), Au1–Cl2 2.2837(18), Au1–Cl3 2.2868(18), Au1–C1 1.954(7), C1–N1 1.143(9), C1–Au1–Cl1 178.4(2), C1–Au1–Cl2 86.78(19), C1–Au1–Cl3 90.8(2), Cl1–Au1–Cl2 91.90(7), Cl2–Au1–Cl3 177.49(7), Au1–C1–N1 176.5(6), C1–N1–C2 178.9(7).

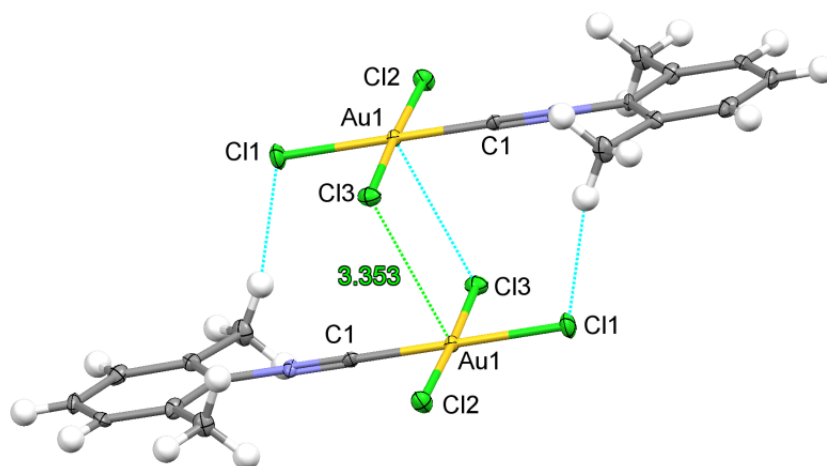


Figure S2. Packing diagram for complex **5**.

DFT calculations for model isocyanide complexes [AuCl₃(CNMe)] and [AuCl(CNMe)]

We carried out theoretical DFT calculations (viz., geometry optimization procedure in gas phase, calculation of vibrational frequencies, and natural bond orbital (NBO) analysis) to compare reactivity of gold(III)- and gold(I)-isocyanide complexes toward nucleophilic attacks using [AuCl₃(CNMe)] and [AuCl(CNMe)] as model species. The composition and energies of the frontier molecular orbitals (FMOs) is one of the main factors determining the reactivity of isocyanide complexes in nucleophilic addition processes, and energy level of first unoccupied MO bearing $\pi^*(\text{C}\equiv\text{N})$ orbitals determine the activation of appropriate ligand (the lower the energy, the higher the activation). The energy level of this MO (viz., LUMO-1, **Figure S3**) in [AuCl₃(CNMe)] (-2.07 eV) is significantly lower than that in [AuCl(CNMe)] (-1.47 eV), thereby simple qualitative MO consideration suggests that the Au(III) center is more potent activator of the isocyanide ligands toward the addition of nucleophiles. Another important factor effecting the reactivity of molecules is the charge distribution on reacting atoms, for our case, the charges on the C atoms of the C \equiv N groups of isocyanide ligands. The calculated NBO charges on these C atoms in [AuCl₃(CNMe)] and [AuCl(CNMe)] are 0.44 and 0.30, respectively. Thus, in terms of electrostatic arguments, the coordination of isocyanide ligand to Au(III) center should facilitate the nucleophilic attack at the C atom of the C \equiv N group. Finally, the $\nu(\text{C}\equiv\text{N})$ vibration is the most analytically important characteristic frequency in the IR spectrum of isocyanide complexes. This frequency can be used as the indicator of the reactivity of these substrates toward nucleophilic attacks (the higher the frequency, the higher the activation).¹⁹ The calculated value of the unscaled normal mode frequency $\nu(\text{C}\equiv\text{N})$ in [AuCl₃(CNMe)] (2389 cm⁻¹) is greater than that in [AuCl(CNMe)] (2321 cm⁻¹). Thus, based on the basis of the criterion $\Delta\nu$, gold(III)-isocyanide complexes more prone toward addition of a nucleophile. Thus, orbital, charge and

frequency arguments reveal that Au(III) center is better activator of CNR ligand in nucleophilic addition processes compare to Au(I).

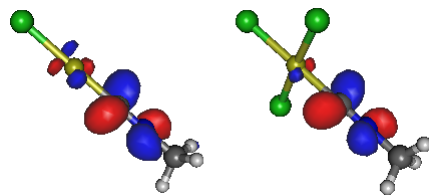
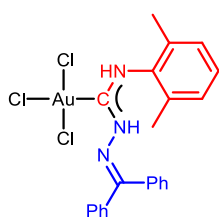


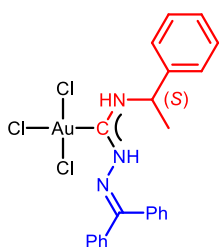
Figure S3. Plots of first unoccupied MOs bearing $\pi^*(\text{C}\equiv\text{N})$ orbitals for $[\text{AuCl}(\text{CNMe})]$ and $[\text{AuCl}_3(\text{CNMe})]$ complexes.

Addition of benzophenone hydrazone to gold(III)-bound isocyanides

Preparation of complexes 14 and 16. A solution of benzophenone hydrazone (**13**, 5 mg, 0.025 mmol) in dry CH₂Cl₂ (0.5 mL) was added to a solution of freshly prepared **5** or **8** (11 mg, 0.025 mmol) in dry CH₂Cl₂ (1 mL) at ca. 25 °C to form a bright orange solution. The reaction mixture was left to stand at RT for ca. 15 min, a change of the reaction color to yellow was noted. Solvent was then removed under a flow of N₂ to form the orange oil that was washed with hexane (two 2-mL portions) and dried in vacuum. Yields: 60% (**14**) and 76% (**16**). Recrystallization of **14** from CDCl₃ at RT under dinitrogen led to deposition of bright yellow crystals of **14** suitable for X-ray diffraction.



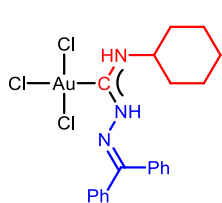
[AuCl₃C(NHXyl)(NHNCPh₂)] (**14**, yellow solid, 60%). Elemental analyses were not conclusive due to slow decomposition of compound at RT. MS (ESI⁺) *m/z*: [M - 3Cl]⁺ calcd. for C₂₃H₂₂N₂Au: 523, found: 523. FT-IR (KBr, selected bands, cm⁻¹): 3284, 3217 (m, N-H), 3012–2885 (w, C-H), 1574 (s, C_{carbene}=N). ¹H NMR (CD₃OD, δ): 7.90 (s, 1H, NH), 7.75 (s, 1H, 2NH), 7.74–7.10 (m, 13H, C_{Ar}H), 2.30 (s, 6H, Me). ¹³C {¹H} NMR (CD₃OD, δ): 136.0, 135.7, 131.7, 131.4, 130.9, 129.5, 129.3, 129.0, 128.9, 128.8, 128.3 and 128.2 (C_{ar}), 16.7 (Me), C_{carbene}=N and C=N signals were not detected due to the fast decomposition of the complex in solution.



[AuCl₃C(NH(S)-CHMePh)(NHNCPh₂)] (**16**, yellow solid, 76%). Elemental analyses were not conclusive due to slow decomposition of compound at RT. MS (ESI⁺) *m/z*: [M - 3Cl]⁺ calcd. for C₂₃H₂₂N₂Au: 523, found 523. FT-IR (KBr, selected bands, cm⁻¹): 3312, 3254 (m, N-H), 3035–2873 (w, C-H), 1571 (s, C_{carbene}=N). ¹H NMR (CD₂Cl₂, δ): 9.08 (s, 1H, NH), 8.34 (d, ³J_{HH} 8.4 Hz, 1H, NH), 7.75–7.25 (m, 15H, C_{Ar}H),

5.67–5.57 (m, 1H, CH), 1.90 (d, $^3J_{\text{HH}}$ 6.9 Hz, 3H, Me). $^{13}\text{C}\{^1\text{H}\}$ NMR (CD_2Cl_2 , δ): 162.7 ($\text{C}_{\text{carbene}}=\text{N}$), 161.9 ($\text{C}=\text{N}$), 139.2, 135.1, 132.0, 131.7, 130.2, 130.0, 129.2, 129.0, 128.8, 128.7, 128.6, 126.9 (12s, C_{ar}), 59.3 (CH), 21.4 (Me);

Preparation of complex 15. A solution of benzophenone hydrazone (**13**, 4.6 mg, 0.025 mmol) in CD_2Cl_2 (0.2 mL) was added to a solution of **6** (8.5 mg) in CD_2Cl_2 (0.2 mL) in an NMR tube giving an orange solution of **15**, whereupon ^1H NMR spectrum was recorded immediately. The pure compound is unstable after solvent evaporation.



[AuCl₃C(NHCy)(NHNCPh₂)] (**15**, NMR yield 76%); ^1H NMR (CD_2Cl_2 , δ): 8.98 (s, 1H, NH), 8.05 (d, $^3J_{\text{HH}}$ 9 Hz, 1H, NH), 7.75–7.31 (m, 10H, $\text{C}_{\text{ar}}\text{H}$), 4.33–4.14 (m, 1H, CH from Cy), 2.32–2.22, 1.94–1.65 and 1.60–1.46 (m, 2+4+4H, CH_2).

Characterization of the prepared carbene complexes 14–16

The ESI $^{+/-}$ -MS spectra of **14** and **16** displayed signals that were attributed to the fragmentation ions $[\text{M} - 3\text{Cl}]^+$, $[\text{M} - 3\text{Cl} + \text{CNR}^1]^+$, and $[\text{M} - \text{CNR}^1 - \text{H}]^-$. The IR spectra of **14** and **16** indicated formation of the carbene moiety, thus, intense absorption at 1574 (**14**) and 1571 cm^{-1} (**16**) was assigned to $\nu(\text{N}-\text{C}_{\text{carbene}})$ and corresponding $\nu(\text{N}-\text{H})$ bands emerge in the range of 3312–3035 cm^{-1} ; $\nu(\text{C}-\text{H})$ stretching bands appeared in the 3035–2873 cm^{-1} range. In the ^1H NMR spectra of **14–16**, resonances of both NH protons were detected in the range of 7.75–9.08 ppm. The aromatic protons were detected as multiplets in the range 7.10–7.75 ppm. The methyl groups of the Xyl fragment appeared as a singlet at 2.30 ppm and CH proton from cyclohexyl group was detected as a broad multiplet in the δ 4.14–4.33 interval. In the ^1H NMR spectrum of **16**, the characteristic signal of the asymmetric CH proton appeared as a multiplet in the 5.57–5.67 ppm range, whereas methyl protons were

detected as a doublet at 1.90 ppm. In the $^{13}\text{C}\{^1\text{H}\}$ NMR spectrum of **16**, two higher frequency signals were found. With the help of $^1\text{H}, ^{13}\text{C}$ -HMBC data, the resonances at δ 162.7 and 161.9 in the ^{13}C NMR spectra of **16** were assigned to $\text{C}_{\text{carbene}}\text{-N}$ and $\text{C}=\text{N}$, correspondingly. To our knowledge, no data on $^{13}\text{C}\{^1\text{H}\}$ NMR of gold(III)-ADC complexes have been previously reported. This δ value for the $\text{C}_{\text{carbene}}=\text{NH}$ ^{13}C signal is lower field relatively to those (199–206 ppm) reported for the series of gold(I)-ADC complexes, *i.e.* $[\text{LAu}\{\text{C}(\text{NH}t\text{-Bu})(\text{NEt}_2)\}]$ ($\text{L} = \text{acac}, \text{C}\equiv\text{CR}, \text{NEt}_3$).²⁰ Also, the observed value of the carbene carbon resonance in **16** is shifted to a lower field, when compared to the corresponding Pd(II) and Pt(II)-ADC complexes also generated via the nucleophilic addition of **13** to an isocyanide in *cis*- $[\text{MCl}_2(\text{CNR}^1)]$ ($\text{M} = \text{Pd}, \text{Pt}; \delta$ 179.7–164.5 ppm).²¹

Although complex **14** possesses low stability in the solid state, we could isolate crystals suitable for X-ray diffraction performed at 150 K in cryo-oil. The asymmetric unit of **14** contains one molecule of the complex and one of chloroform, and respective bond lengths and angles are discussed in the manuscript.

The solid-state structure of **14** exhibits intermolecular T-shaped $\text{C-H}\cdots\pi$ interactions involving both the C26–H8 and the C23–H10 bonds of every molecule and the C3–C8 phenyl rings of adjacent ones (2.847 and 2.743 Å, in this order); such interactions give rise to infinite chains along the crystallographic *a* axis (**Figure S4A**). Additionally, the N1–H20 protons are involved in bifurcated intermolecular hydrogen-bonding to the Cl1 and Cl3 atoms of a neighboring molecule, assembling them in pairs (**Figure S4B**). [$\text{H}\cdots A$ and $D\text{-H}\cdots A$ (Å, °): N1–H20 \cdots Cl1 2.68(7), 140(6), N1–H20 \cdots Cl3 2.81(7), 146(6)].

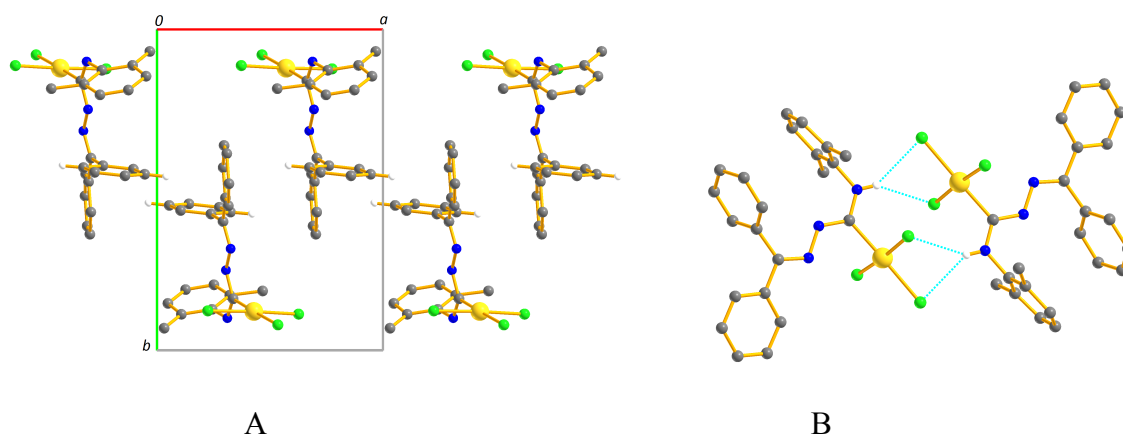


Figure S4. Intermolecular T-shaped C–H \cdots π (A) and N–H \cdots Cl (B) interactions in the molecular structure of **14**. H-atoms not involved in such interactions are omitted for clarity.

Reaction of [AuCl₃(CNR¹)] (**5–8**) with amines

Reaction of complexes **5–8** with achiral primary (benzylamine **9**, α -methylbenzylamine **11**) and secondary (morpholine **10**) and chiral amine (α -(*R*)-methylbenzylamine (*R*)-**11**) was studied at different conditions (*i.e.* varying temperature, solvent and molar ratio of the reagents).

Therefore, when solution of one or two equiv of **9** or **10** (in dry CH₂Cl₂) was added to freshly prepared **5–8** in CH₂Cl₂ (at -74 °C), a bright orange solution was formed. When warmed to the RT, color of the solution changed to yellow and white precipitate was formed. In each case, reaction mixture contained partially dissolved hydrochloride of the corresponding amine and product of reduction of the starting complex in solution (to **1–4**, respectively) along with some yet unidentified species. However, in the ESI-MS spectra, traces of diaminocarbene species formed via nucleophilic addition of **9** or **10** to **1–4** (formed during reduction of **5–8**), were detected by the ESI-MS.

To increase the life time of intermediates/products in the reaction of amines **9** or **10** with **5–8** and minimize the influence of solvent and air, we studied these reactions in dried degassed aprotic nonpolar solvent (e.g. toluene, which was chosen for its relatively high ability to dissolve **5–8** and low melting temperature, *i.e.* ca. -95 °C) under N₂ atmosphere at -74 °C. When solution of **9** or emulsion of **10** in dry toluene was added to the solution of **5–8** at -74 °C, a bright orange mixture was formed. When warmed to the RT, a white precipitate of the corresponding amine hydrochloride was generated (detected by ESI-MS, IR and NMR spectroscopy). Evaporation of the solvent from a yellow solution formed after precipitation of the hydrochloride gave an oily residue which contained product of reduction of the starting complex **5–8** in solution to **1–4** along with some yet unidentified products.

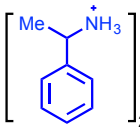
When more sterically hindered and basic amine, such as α -methylbenzylamine (**11**) was used in a place of nucleophile, its reaction with any of **5–8** (1:1 ratio) in CH₂Cl₂ at -74 °C

led to the formation of the complex salt **12** (Scheme 2, Figure S5) in ca. 21–30% yield based on Au. Change of the ratio gold(III)-isocyanide:amine to 2:3 increased the yield of **12** to ca. 40–42%. In the solution, the presence of **12**•HCl, respective gold(I)-isocyanide complexes **1–4**, alongside with 1-phenylethan-1-imine (see Figure S6 for the HR-ESI-MS of this compound) and trace amounts of some yet unidentified species, were established using ESI-MS, FT-IR, and ¹H NMR spectroscopy. Compound **12** precipitated from the reaction mixture as a bright yellow crystalline solid. Change of the solvent for undried MeCN or increasing of the temperature to 20–25 °C led to decrease of the yield of **12** to 5–10%. When dry toluene was used as a solvent and reaction was performed under N₂ atmosphere, complex salt **12** was not formed but a white precipitate of **11**•HCl was recovered in ca. 46% yield. When complex to amine ratio equal to 1:2 was used, complex salt **12** was also formed with a decreased yield (5–13%), and it was contaminated with excess of **11**•HCl. In the ESI-MS spectra, traces of the diaminocarbene species formed via nucleophilic addition of **11** to **1–4** (formed during reduction of **5–8**) were detected.

Reaction of optically pure α -(*R*)-methylbenzylamine ((*R*)-**11**, 1 equiv) with **5–8** in dry CH₂Cl₂ at –74 °C under N₂ afforded yellow oily residue (see below). Dropwise addition of CDCl₃ to the latter led to precipitation of orange crystals of {(*R*)-H₃NCHMePh}₂[AuCl₄](Cl) ((*R*)-**12**) that were stable enough for X-ray diffraction.

Reaction of 11 with 5–8. A solution of α -methylbenzylamine (**11**) or (*R*)-(+)- α -methylbenzylamine ((*R*)-**11**) (9 mg, 0.075 mmol) in CH₂Cl₂ (0.5 mL) and solution of freshly prepared **5–8** (0.025 mmol) in CH₂Cl₂ (1 mL) were cooled to –74° in acetone-liquid nitrogen cooling bath and were mixed to form a bright orange solution. The reaction mixture was immediately analyzed by HR ESI-MS (see Supporting information) allowing the detection of gold(I)-isocyanides **1–4** and 1-phenylethan-1-imine present. Afterwards, reaction mixture was left to warm up to RT until the

solution turned yellow (for ca. 40 min). After removal of the solvent under a flow of N₂ the mixture of crystalline solid and an oily residue (**12**) or an oily residue (**(R)-12**) was obtained. It was washed with cold CHCl₃ (two 2-mL portions) to give bright yellow crystalline powder of **12** (or **(R)-12**) suitable for X-ray diffraction studies, that was further dried under dinitrogen at RT. Yield was 40–42% based on the metal. Analytical data obtained for **12** and **(R)-12** were comparable. Application of the other solvents (benzene, toluene, tetrahydrofuran, diethyl ether) in the place of CH₂Cl₂ led to a broad mixture of yet unidentified products.


 $\left[\text{Me-CH(NH}_3^+) \text{-C}_6\text{H}_4 \right]_2 [\text{AuCl}_4]\text{Cl}$ (**(R)-12**, bright-yellow crystals, 42%). Anal. calcd for C₁₆H₂₄N₂Cl₆Au•0.5CH₂Cl₂: C 29.97, H 3.81, N 4.24; found: C 30.38, H 3.72, N 4.25%. HRMS (ESI⁺) *m/z*: [NH₃CHMePh]⁺ calcd. for C₈H₁₂N: 122.0964, found: 122.0968; [2(NH₃CHMePh) + Cl]⁺ calcd. for C₁₆H₂₄N₂Cl: 279.1628, found: 279.1623. HRESI⁻-MS, *m/z*: [AuCl₄]⁻ calcd. for AuCl₄: 338.8396, found: 338.8385. FT-IR (KBr, selected bands, cm⁻¹): 3199 and 3151 (s, N–H), 3000 and 2919 (s, C–H), 1592, 1581, 1494 and 1385 (s, C=C), 763 and 698 (s, δ(C–H)). ¹H NMR (CD₂Cl₂, δ): 7.73 (s, br, 2*H*, NH₂), 7.57–7.40 (m, 5*H*, C_{ar}H), 4.58 (m, br, 1*H*, CH), 1.75 (d, 3*H*, ³J_{HH} 6.4 Hz, Me). ¹³C {¹H} NMR (CD₂Cl₂, δ): 136.8 (C_{ar}), 129.6, 129.4 and 127.1 (C_{ar}H), 52.8 (CH), 20.3 (Me).

Characterization of 12. Complex salts **12** and **(R)-12** were characterized by elemental analyses, HRESI-MS, IR and NMR spectroscopic techniques and X-ray diffraction for **(R)-12**. Compounds **12** and **(R)-12** gave satisfactory results of the C, H and N elemental analyses that are consistent with the proposed formulations. For both complex **12** and **(R)-12**, signals due to [NH₃CHMePh]⁺ and [NH₃CHMePh + Cl]⁺ in the HRESI⁺-MS, and due to [AuCl₄]⁻ in the HRESI⁻-MS, were observed. The IR spectra of **12** and **(R)-12** contained four strong bands

in the range 1385–1592 cm^{-1} that were attributed to $\nu(\text{C}=\text{C})$ stretching vibrations, and two strong bands in the 3151–3199 range due to $\nu(\text{N}-\text{H})$. Bands in the 2919–3000 cm^{-1} range are characteristic for $\nu(\text{C}-\text{H})$ stretches, while corresponding $\delta(\text{C}-\text{H})$ were detected in the 698–763 range. Both ^1H and $^{13}\text{C}\{^1\text{H}\}$ NMR spectra show all expected resonances and support the formulation of **12** and (*R*)-**12**.

The structure of (*R*)-**12** was determined by single-crystal X-ray diffraction (**Figure S5**). The crystal of (*R*)-**12** is built up from two protonated α -methylbenzylamine cations, one $[\text{AuCl}_4]^-$ anion and one Cl^- anion disordered by two positions. In both cations all bond lengths and angles are equal within 3σ . $[\text{AuCl}_4]^-$ possesses a square-planar geometry around the metal center. All Au–Cl distances (2.273(5)–2.280(5) Å) have typical values for Au–Cl, and are as observed in related Au(III) and Au(I) compounds.^{14, 16a-e, 22}

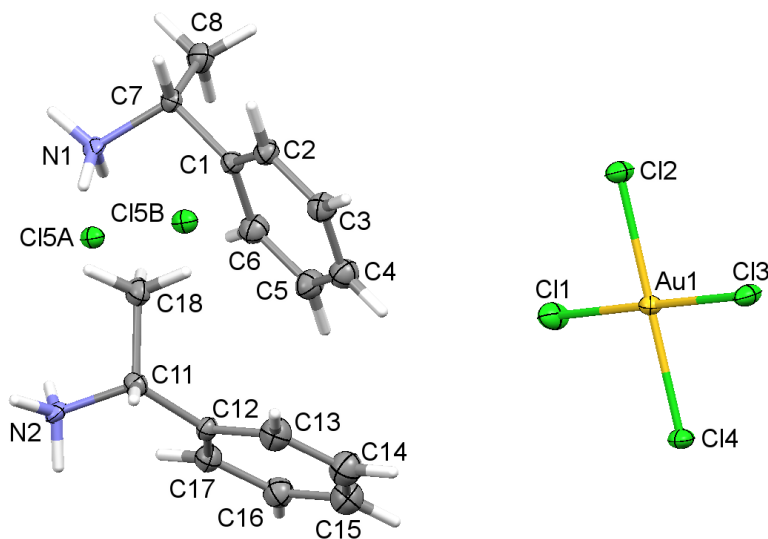


Figure S5. Crystal structure of (*R*)-**12** with atomic numbering scheme (hydrogen labels are removed for simplicity). Thermal ellipsoids are drawn at the 11% probability level. Selected bond lengths (Å) and angles ($^\circ$): Au1–Cl1 2.278(5), Au1–Cl2 2.273(5), Au1–Cl3 2.279(4), Au1–Cl4 2.280(5), C7–N1 1.143(9), C11–N2 1.143(9), Cl2–Au1–Cl1 89.8(2), Cl2–Au1–Cl4

179.15(19), Cl1–Au1–Cl4 90.8(2), Cl2–Au1–Cl3 90.68(19), Cl1–Au1–Cl3 179.5(13), C4–Au1–Cl3 88.7(2).

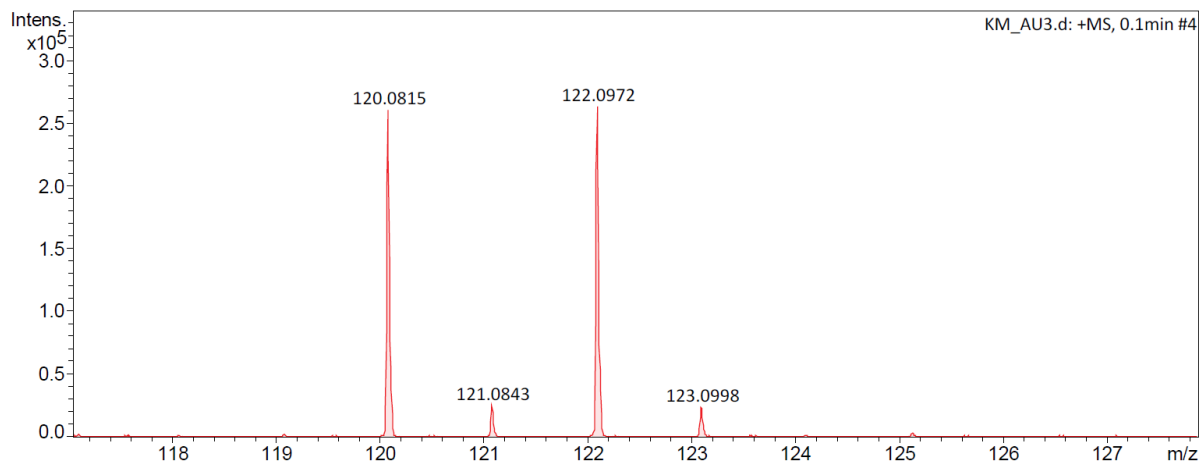


Figure S6. HR-ESI⁺-MS of 1-phenylethan-1-imine (120.0815 [M + H]⁺ [calcd. 120.0813]) and 1-phenylethan-1-amine (122.0972 [M + H]⁺ [calcd. 122.0970]) detected in the reaction mixture.

Reactions of $[\text{AuCl}_3(\text{CNR}^1)]$ with other NH-nucleophiles

We have tested complexes **5–8** in the reactions with other nucleophiles, namely: *p*-chloroaniline, benzophenone imine, methylhydrazine, benzylhydrazine, carbohydrazide, benzhydrazide and 1,3-iminoisoindolinone. All the reactions studied led to decomposition of the starting complexes forming either metal gold or the corresponding $[\text{AuCl}(\text{CNR}^1)]$ complexes (in the cases of *p*-chloroaniline, benzophenone imine, benzhydrazide and 1,3-iminoisoindolinone). No formation of the carbene products was observed for any of those.

It should be mentioned that all nucleophiles (namely, *p*-chloroaniline, benzophenone imine, methylhydrazine, benzylhydrazine, carbohydrazide, benzhydrazide and 1,3-iminoisoindolinone) used in this work were tested in the reaction with $[\text{AuCl}(\text{CNR}^1)]$ species and in all the cases nucleophilic addition did not occur in CH_2Cl_2 even after 6 h at 40 °C but led to partial decomposition of the starting material releasing metal-containing black precipitate.

Theoretical evaluation of the bonding situation in dimers **5**, **14**, and **(R)-12**

Inspection of the crystallographic data suggests the presence of short contacts Au•••Au (aurophilic interactions) in dimers **5**, **14**, and **(R)-12** in solid state (for more detailed discussion about the identification of such contacts, see Ref. ²³). Indeed, the interatomic distances between the gold atoms in these associates (3.98, 4.30, and 4.21 Å, respectively) falls within the range of sum of their van der Waals radii defined by different approaches (the smallest {3.32 Å} proposed by Bondi²⁴, and the largest {4.86 Å} proposed by Allinger et al.²⁵). In order to study the bonding situation and to confirm or deny assumption about the existence of aurophilic interactions in dimers **5**, **14**, and **(R)-12** we carried out theoretical DFT calculations and performed topological analysis of the electron density distribution within the formalism of Bader's theory (QTAIM analysis). The results are summarized in **Table S2**, the contour line diagrams of the Laplacian distribution $\nabla^2\rho(\mathbf{r})$, bond paths, and selected zero-flux surfaces for dimers **5**, **14**, and **(R)-12** are shown in **Figure S7**.

Table S2. Values of the density of all electrons – $\rho(\mathbf{r})$, Laplacian of electron density – $\nabla^2\rho(\mathbf{r})$, energy density – H_b , potential energy density – $V(\mathbf{r})$, and Lagrangian kinetic energy – $G(\mathbf{r})$ (Hartree) at the bond critical points (3, –1), corresponding to different contacts in dimers **5**, **14**, and **(R)-12**, bond lengths (l , Å) and appropriate Wiberg bond indices (WI) as well as energies of these interactions E_{int} (kcal/mol), defined by two methods.^a

Contact	$\rho(\mathbf{r})$	$\nabla^2\rho(\mathbf{r})$	H_b	$V(\mathbf{r})$	$G(\mathbf{r})$	l	WI	E_{int}^b	E_{int}^c
5									
Au•••Au	BCP not found					3.98	0.02	---	---
	<i>BCP not found</i>						<i>0.01</i>	---	---
Au•••Cl	0.014	0.045	0.001	-0.009	0.010	3.35	0.06	2.8	2.7
	<i>0.013</i>	<i>0.041</i>	<i>0.001</i>	<i>-0.007</i>	<i>0.009</i>		<i>0.06</i>	<i>2.2</i>	<i>2.4</i>
Au–Cl	0.107	0.196	-0.035	-0.118	0.084	2.29	0.75	37.0	22.6
	<i>0.101</i>	<i>0.226</i>	<i>-0.030</i>	<i>-0.110</i>	<i>0.083</i>		<i>0.71</i>	<i>34.5</i>	<i>22.3</i>
14									
Au•••Au	BCP not found					4.30	0.01	---	---
	<i>BCP not found</i>						<i>0.01</i>	---	---
Au•••Cl	0.010	0.034	0.001	-0.006	0.007	3.51	0.05	1.9	1.9
	<i>0.010</i>	<i>0.028</i>	<i>0.001</i>	<i>-0.005</i>	<i>0.006</i>		<i>0.05</i>	<i>1.6</i>	<i>1.6</i>
Au–Cl	0.103	0.201	-0.032	-0.115	0.082	2.30	0.72	36.1	22.1
	<i>0.097</i>	<i>0.230</i>	<i>-0.029</i>	<i>-0.107</i>	<i>0.082</i>		<i>0.68</i>	<i>33.6</i>	<i>22.1</i>
(R)-12									
Au•••Au	BCP not found					4.21	0.02	---	---
	<i>BCP not found</i>						<i>0.01</i>	---	---
Au•••Cl	0.008	0.027	0.001	-0.004	0.005	3.63	0.03	1.3	1.4
	<i>0.008</i>	<i>0.022</i>	<i>0.001</i>	<i>-0.004</i>	<i>0.005</i>		<i>0.03</i>	<i>1.3</i>	<i>1.4</i>
Au–Cl	0.107	0.208	-0.034	-0.120	0.086	2.28	0.76	37.7	23.2
	<i>0.101</i>	<i>0.232</i>	<i>-0.031</i>	<i>-0.111</i>	<i>0.085</i>		<i>0.71</i>	<i>34.8</i>	<i>22.9</i>

^a Relativistic approach – normal text, non-relativistic – italics (for details see **Computational Details** section in the main text).

^b $E_{\text{int}} = -V(\mathbf{r})/2$ (see Ref. ²⁶)

^c $E_{\text{int}} = 0.429G(\mathbf{r})$ (see Ref. ²⁷)

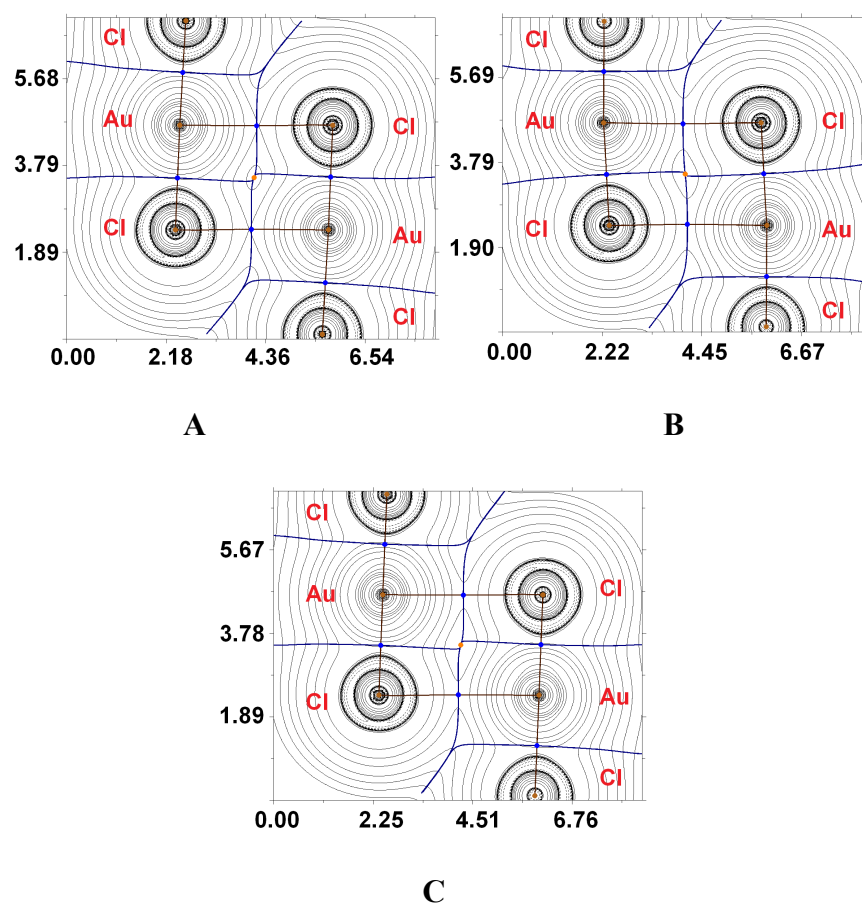


Figure S7. Contour line diagrams of the Laplacian distribution $\nabla^2\rho(\mathbf{r})$, bond paths and selected zero-flux surfaces for dimers **5** (A), **14** (B), and **(R)-12** (C). Bond critical points (3, -1) are shown in blue, nuclear critical points (3, -3) – in pale brown, ring critical points (3, +1) – in orange, length unit – Å.

The QTAIM analysis shows the presence of two bond critical points (3, -1) (BCPs) for covalent bonds Au–Cl and two BCPs for Au•••Cl non-covalent interactions, but no BCPs for Au•••Au contacts in all studied dimers. Thus, our assumption about the presence of aurophilic interactions in dimers **5**, **14**, and **(R)-12** is not confirmed theoretically from the QTAIM formalism’s point of view. The magnitudes of the electron density, values of the Laplacian and energy density, the ratio $-G(\mathbf{r})/V(\mathbf{r})$ in BCPs for Au–Cl and Au•••Cl contacts as well as

appropriate Wiberg bond indices (WI) are typical for covalent bonds M–L in coordination complexes and for non-covalent electrostatic interactions, respectively. We have defined energies for these contacts according to the procedures proposed by Espinosa et al.²⁶ and Vener et al.²⁷ (**Table S2**), and one can state that the relativistic and non-relativistic approaches gives very similar estimates. Results of theoretical calculations led to a conclusion that weak Au•••Cl non-covalent electrostatic interactions and not the aurophilic interactions are responsible for the stabilization of dimeric associates **5**, **14**, and (**R**)-**12** in solid state.

Table S3. Cartesian atomic coordinates of model species.

Atom	X	Y	Z
5			
Au	6.272028	5.110382	5.924476
Cl	6.779241	5.185342	8.134593
Cl	4.037719	4.942848	6.364831
Cl	8.486836	5.297713	5.388415
N	5.446292	5.079251	2.941760
C	5.789288	5.071058	4.031420
C	5.000180	5.094270	1.616845
C	3.603426	5.157078	1.425433
C	3.227349	5.148886	0.108004
H	2.299213	5.180290	-0.091963
C	4.116570	5.095635	-0.949576
H	3.786450	5.092905	-1.840338
C	5.477093	5.046481	-0.727153
H	6.084116	5.010981	-1.456444
C	5.948444	5.047847	0.591346
C	7.414665	4.967289	0.920704
H	7.696192	5.796081	1.362342
H	7.929359	4.845769	0.095171
H	7.573859	4.208132	1.519535
C	2.641744	5.239001	2.545034
H	2.809619	4.505787	3.172738
H	1.728742	5.168001	2.196429
H	2.750179	6.096466	3.006990
Au	7.920225	8.543518	4.768945
Cl	7.413012	8.468558	2.558829
Cl	10.154534	8.711052	4.328590
Cl	5.705417	8.356187	5.305006
N	8.745961	8.574649	7.751661
C	8.402965	8.582842	6.662002
C	9.192073	8.559630	9.076576
C	10.588827	8.496822	9.267988
C	10.964904	8.505014	10.585418
H	11.893040	8.473610	10.785385
C	10.075683	8.558265	11.642997
H	10.405803	8.560995	12.533759
C	8.715160	8.607419	11.420574
H	8.108137	8.642919	12.149865
C	8.243809	8.606053	10.102075
C	6.777588	8.686611	9.772718
H	6.496061	7.857819	9.331080
H	6.262894	8.808131	10.598250
H	6.618394	9.445768	9.173886
C	11.550509	8.414899	8.148387

H	11.382634	9.148113	7.520683
H	12.463511	8.485899	8.496993
H	11.442074	7.557434	7.686431
14			
Au	5.667245	1.717367	1.123982
Cl	7.641980	1.744611	2.240572
Cl	4.474517	1.126512	3.030607
Cl	3.758207	1.599877	-0.153261
N	7.022930	3.540305	-0.667115
N	6.751745	4.489589	0.305356
C	7.766839	1.807755	-2.621781
C	6.693992	2.276012	-0.505685
C	7.108252	5.692868	-0.001945
C	6.935988	6.738641	1.024984
C	7.054932	8.080977	0.694344
H	7.209054	8.333552	-0.208109
C	6.952131	9.055803	1.672649
H	7.023690	9.973870	1.437312
C	6.745327	8.695387	2.983540
H	6.681724	9.366555	3.652600
C	6.629263	7.362983	3.331684
H	6.485938	7.118922	4.238027
C	6.721513	6.392415	2.361159
H	6.637520	5.477186	2.602331
C	7.733204	6.024904	-1.332285
C	9.090523	6.179571	-1.458706
H	9.640895	6.132745	-0.684619
C	9.672362	6.403766	-2.697633
H	10.613653	6.505932	-2.775431
C	8.870891	6.474714	-3.812085
H	9.257918	6.630800	-4.665914
C	7.514331	6.322886	-3.697333
H	6.966972	6.362617	-4.471420
C	6.937261	6.110042	-2.454516
H	5.994966	6.024904	-2.376718
N	7.011497	1.423217	-1.448981
C	7.056744	2.434935	-3.658434
C	7.813679	2.891840	-4.747601
H	7.387841	3.354421	-5.459450
C	9.092101	2.684672	-4.788445
H	9.562967	2.984073	-5.556697
C	9.818418	2.064587	-3.800415
H	10.756576	1.946813	-3.891827
C	9.127612	1.593492	-2.615946
C	9.824350	0.976244	-1.482045

H	9.640761	1.487070	-0.667115
H	10.789921	0.971988	-1.655145
H	9.509498	0.055339	-1.367294
C	5.584959	2.620819	-3.640930
H	5.303573	3.083400	-4.457805
H	5.333203	3.155767	-2.859064
H	5.144822	1.746740	-3.592306
H	7.471912	3.760244	-1.361459
H	6.741127	0.681101	-1.400358
Au	4.378155	-1.717367	-1.123982
Cl	2.403420	-1.744611	-2.240572
Cl	5.570883	-1.126512	-3.030607
Cl	6.287193	-1.599877	0.153261
N	3.022470	-3.540305	0.667115
N	3.293655	-4.489589	-0.305356
C	2.278561	-1.807755	2.621781
C	3.351408	-2.276012	0.505685
C	2.937148	-5.692868	0.001945
C	3.109412	-6.738641	-1.024984
C	2.990468	-8.080977	-0.694344
H	2.836346	-8.333552	0.208109
C	3.093269	-9.055803	-1.672649
H	3.021710	-9.973870	-1.437312
C	3.300073	-8.695387	-2.983540
H	3.363676	-9.366555	-3.652600
C	3.416137	-7.362983	-3.331684
H	3.559462	-7.118922	-4.238027
C	3.323887	-6.392415	-2.361159
H	3.407880	-5.477186	-2.602331
C	2.312196	-6.024904	1.332285
C	0.954877	-6.179571	1.458706
H	0.404505	-6.132745	0.684619
C	0.373038	-6.403766	2.697633
H	-0.568253	-6.505932	2.775431
C	1.174509	-6.474714	3.812085
H	0.787482	-6.630800	4.665914
C	2.531069	-6.322886	3.697333
H	3.078428	-6.362617	4.471420
C	3.108139	-6.110042	2.454516
H	4.050434	-6.024904	2.376718
N	3.033903	-1.423217	1.448981
C	2.988656	-2.434935	3.658434
C	2.231721	-2.891840	4.747601
H	2.657559	-3.354421	5.459450
C	0.953299	-2.684672	4.788445

H	0.482433	-2.984073	5.556697
C	0.226982	-2.064587	3.800415
H	-0.711176	-1.946813	3.891827
C	0.917788	-1.593492	2.615946
C	0.221050	-0.976244	1.482045
H	0.404639	-1.487070	0.667115
H	-0.744521	-0.971988	1.655145
H	0.535902	-0.055339	1.367294
C	4.460441	-2.620819	3.640930
H	4.741827	-3.083400	4.457805
H	4.712197	-3.155767	2.859064
H	4.900578	-1.746740	3.592306
H	2.573488	-3.760244	1.361459
H	3.304273	-0.681101	1.400358
(R)-12			
Cl	9.160024	3.548348	16.208939
Cl	10.163459	1.210961	18.174710
Cl	11.053819	3.434226	20.353594
Cl	10.085108	5.758933	18.400360
Au	10.108791	3.481777	18.280333
Cl	8.647176	3.548348	23.799961
Cl	7.643741	1.210961	21.834190
Cl	6.753381	3.434226	19.655306
Cl	7.722092	5.758933	21.608540
Au	7.698409	3.481777	21.728567
[AuCl ₃ (CNMe)]			
Cl	1.225501	1.476962	-2.703958
Au	0.113427	0.515475	-0.930022
Cl	2.077224	0.480478	0.359765
C	-0.854049	-0.323738	0.619701
Cl	-1.908000	0.496599	-2.126908
N	-1.408344	-0.803541	1.505007
C	-2.084562	-1.393882	2.601081
H	-2.753363	-0.656893	3.049631
H	-2.665945	-2.247397	2.247206
H	-1.352302	-1.725208	3.339490
[AuCl(CNMe)]			
Au	-0.022973	0.000487	0.000603
Cl	2.273349	-0.001999	0.000613
C	-1.981890	0.001730	0.000146
N	-3.140531	0.001712	-0.000852
C	-4.554636	0.000309	-0.001954
H	-4.921004	-0.728879	-0.727873
H	-4.923476	0.992693	-0.270432
H	-4.922936	-0.264095	0.991701

References for Supplementary Information

1. A. S. K. Hashmi, T. Hengst, C. Lothschutz and F. Rominger, *Adv. Synth. Catal.*, 2010, **352**, 1315–1337.
2. *Bruker APEX2 & SAINT. Bruker, AXS Inc., Madison, Wisconsin, USA*, 2004.
3. G. M. Sheldrick, *SADABS – Bruker AXS scaling and absorption correction*, 2008.
4. L. Farrugia, *J. Appl. Crystallogr.*, 1999, **32**, 837–838.
5. Y. Zhao and D. G. Truhlar, *Theor. Chem. Acc.*, 2007, **120**, 215–241.
6. M. J. T. Frisch, G. W.; Schlegel, H. B.; Scuseria, G. E.; Robb, M. A.; Cheeseman, J. R.; Scalmani, G.; Barone, V.; Mennucci, B.; Petersson, G. A.; Nakatsuji, H.; Caricato, M.; Li, X.; Hratchian, H. P.; Izmaylov, A. F.; Bloino, J.; Zheng, G.; Sonnenberg, J. L.; Hada, M.; Ehara, M.; Toyota, K.; Fukuda, R.; Hasegawa, J.; Ishida, M.; Nakajima, T.; Honda, Y.; Kitao, O.; Nakai, H.; Vreven, T.; Montgomery, J. A., Jr.; Peralta, J. E.; Ogliaro, F.; Bearpark, M.; Heyd, J. J.; Brothers, E.; Kudin, K. N.; Staroverov, V. N.; Kobayashi, R.; Normand, J.; Raghavachari, K.; Rendell, A.; Burant, J. C.; Iyengar, S. S.; Tomasi, J.; Cossi, M.; Rega, N.; Millam, J. M.; Klene, M.; Knox, J. E.; Cross, J. B.; Bakken, V.; Adamo, C.; Jaramillo, J.; Gomperts, R.; Stratmann, R. E.; Yazyev, O.; Austin, A. J.; Cammi, R.; Pomelli, C.; Ochterski, J. W.; Martin, R. L.; Morokuma, K.; Zakrzewski, V. G.; Voth, G. A.; Salvador, P.; Dannenberg, J. J.; Dapprich, S.; Daniels, A. D.; Farkas, Ö.; Foresman, J. B.; Ortiz, J. V.; Cioslowski, J.; Fox, D. J.. *Gaussian 09, Revision C.01, Gaussian, Inc., Wallingford CT*, 2010.
7. I. V. Alabugin, K. M. Gilmore and P. W. Peterson, *Wiley Interdisciplinary Reviews: Comp. Mol. Sci.*, 2011, **1**, 109–141.
8. (a) F. E. Jorge, A. Canal Neto, G. G. Camiletti and S. F. Machado, *J. Chem. Phys.*, 2009, **130**, 064108; (b) A. Canal Neto and F. E. Jorge, *Chem. Phys. Lett.*, 2013, 158–162; (c) C. L. Barros, P. J. P. de Oliveira, F. E. Jorge, A. Canal Neto and M. Campos, *Mol. Phys.*, 2010, **108**, 1965–1972.

9. D. Andrae, U. Häußermann, M. Dolg, H. Stoll and H. Preuß, *Theor. Chim. Acta*, 1990, 123–141.
10. R. F. W. Bader, *Chem. Rev.*, 1991, **91**, 893–928.
11. T. Lu and F. Chen, *J. Comput. Chem.*, 2012, **33**, 580–592.
12. E. D. Glendening, C. R. Landis and F. Weinhold, *Wiley Interdisciplinary Reviews: Comp. Mol. Sci.*, 2012, **2**, 1–42.
13. (a) J. Wilton-Ely, H. Ehlich, A. Schier and H. Schmidbaur, *Helv. Chim. Acta*, 2001, **84**, 3216–3232; (b) R. Heathcote, J. A. S. Howell, N. Jennings, D. Cartlidge, L. Cobden, S. Coles and M. Hursthouse, *Dalton Trans.*, 2007, 1309–1315.
14. D. Schneider, O. Schuster and H. Schmidbaur, *Organometallics*, 2005, **24**, 3547–3551.
15. (a) A. W. Addison, N. T. Rao, J. Reedijk, J. van Rijn and G. C. Verschoor, *J. Chem. Soc., Dalton Trans.*, 1984, 1349–1356; (b) L. Yang, D. R. Powell and R. P. Houser, *Dalton Trans.*, 2007, 955–964.
16. (a) S. Gaillard, A. M. Z. Slawin, A. T. Bonura, E. D. Stevens and S. P. Nolan, *Organometallics*, 2010, **29**, 394–402; (b) S. F. Zhu, R. X. Liang, L. J. Chen, C. Wang, Y. W. Ren and H. F. Jiang, *Tetrahedron Lett.*, 2012, **53**, 815–818; (c) G. Bandoli, D. A. Clemente, Marangon G. and C. L., *J. Chem. Soc.-Dalton Trans.*, 1973, 886–889; (d) R. J. Staples, T. Grant, J. P. Fackler and A. Elduque, *Acta Crystallogr. Sect. C-Cryst. Struct. Commun.*, 1994, **50**, 39–40; (e) T. S. Teets and D. G. Nocera, *J. Am. Chem. Soc.*, 2009, **131**, 7411–7420; (f) H. Ecken, M. M. Olmstead, B. C. Noll, S. Attar, B. Schlyer and A. L. Balch, *J. Chem. Soc.-Dalton Trans.*, 1998, 3715–3720; (g) R. Y. Liao, T. Mathieson, A. Schier, R. J. F. Berger, N. Runeberg and H. Schmidbaur, *Z.Naturforsch.(B)*, 2002, **57**, 881–889.
17. (a) V. Y. Kukushkin, *Russ J Inorg Chem (Engl Transl)*, 1988, **33**, 1085–1089; (b) J. A. Davies, C. M. Hockensmith, V. Y. Kukushkin and Y. N. Kukushkin, *Synthetic Coordination Chemistry: Principles and Practice*, World Scientific Pub Co Inc, Singapore-New Jersey,

- 1997; (c) J. A. Vicente, A. Arcas, J. M. Fernández-Hernández, D. Bautista and P. G. Jones, *Organometallics*, 2005, **24**, 2516–2527; (d) K. M. Anderson and A. G. Orpen, *Chem. Commun.*, 2001, 2682–2683.
18. H. F. Allen, O. Kennard, D. G. Watson, L. Brammer, A. Guy Orpen and T. Taylor, *J. Chem. Soc. Perkin Trans 2*, 1987, **1987**, S1–S19.
19. R. A. Michelin, A. J. L. Pombeiro and M. F. C. Guedes da Silva, *Coord. Chem. Rev.*, 2001, **218**, 75–112.
20. J. Vicente, M. T. Chicote, M. D. Abrisqueta, M. M. Alvarez-Falcón, F. J. Hernández, M. C. R. d. Arellano and P. G. Jones, *Organometallics*, 2003, **22**, 4327–4333.
21. K. V. Luzyanin, M. F. C. Guedes da Silva, V. Y. Kukushkin and A. J. L. Pombeiro, *Inorg. Chim. Acta*, 2009, **362**, 833–838.
22. H. Ecken, M. M. Olmstead, B. C. Noll, S. Attar, B. Schlyer and A. L. Balch, *J. Chem. Soc.-Dalton Trans.*, 1998, 3715–3720.
23. A. N. Chernyshev, M. V. Chernysheva, P. Hirva, V. Y. Kukushkin and M. Haukka, *Dalton Trans.*, 2015, 14523–14531.
24. (a) A. Bondi, *J. Phys. Chem.*, 1964, **68**, 441–451; (b) A. Bondi, *J. Phys. Chem.*, 1966, **70**, 3006–3007.
25. N. L. Allinger, X. Zhou and J. Bergsma, *J. Mol. Struct. (THEOCHEM)*, 1994, **312**, 69–83.
26. E. Espinosa, E. Molins and C. Lecomte, *Chem. Phys. Lett.*, 1988, **285**, 170–173.
27. M. V. Vener, A. N. Egorova, A. V. Churakov and V. G. Tsirelson, *J. Comput. Chem.*, 2012, **33**, 2303–2309.